arXiv:1206.4574v1 [nucl-th] 20 Jun 2012

Neutron-^{3}H scattering above the four-nucleon breakup threshold

A. Deltuva and A. C. Fonseca
Centro de Física Nuclear da Universidade de Lisboa, P-1649-003 Lisboa, Portugal

(Received June 20, 2012)

The four-body equations of Alt, Grassberger and Sandhas are solved for the neutron-^{3}H scattering at energies above the four-nucleon breakup threshold. The accuracy and practical applicability of the employed complex energy method is significantly improved by the use of integration with the special weights. This allows to obtain fully converged results with realistic nuclear interactions. A satisfactory description of the existing neutron-^{3}H elastic scattering data is obtained.

PACS numbers: 21.45.+v, 21.30.-x, 24.70.+s, 25.10.+s

The four-nucleon reactions is an ideal but also highly challenging field to test few-nucleon interaction models. The problem of elastic nucleon-trinucleon scattering below the inelastic threshold has already been solved with high accuracy using several *ab initio* methods with realistic nuclear potentials. These methods include the hyperspherical harmonics (HH) expansion [1–3], the Faddeev-Yakubovsky (FY) equations [4] for the wave function components in the coordinate space [5, 6], and the Alt, Grassberger and Sandhas (AGS) equations [7, 8] for the transition operators in the momentum space [9–11]. A recent benchmark [12] reported a good agreement between the HH, FY, and AGS techniques for the neutron-^{3}H (n-^{3}H) and proton-^{3}He (p-^{3}He) scattering. Furthermore, deuteron-deuteron (d-d) collisions, including the transfer reactions to p-^{3}H and n-^{3}He final states, have been calculated using the resonating-group method (RGM) [13] and the AGS framework [14, 15]. However, also these calculations were limited to energies below the three-cluster breakup threshold. At higher energies, especially above the four-body breakup threshold, the asymptotic boundary conditions in the coordinate space become nontrivial due to open two-, three- and four-cluster channels. In the momentum-space framework one is faced with a very complicated structure of singularities in the kernel of integral equations. Formally, these difficulties can be avoided by rotation to complex coordinates [16] or continuation to complex energy [17, 18] that lead to bound-state like boundary conditions and nonsingular kernels. However, technical complications may arise in practical calculations. Indeed, the applications to the four-nucleon scattering so far have been very limited [19, 20] and none of them uses realistic interactions. On the other hand, the no-core shell model RGM [21] includes in the model space only the ground state of the three-nucleon system which is insufficient. In Ref. [22] this shortcoming was partially corrected by adjusting the predictions to the experimental data.

The aim of the present work is to overcome the above limitations by performing realistic well-converged four-nucleon scattering calculations above the four-body breakup threshold. We use the complex energy method [17] but introduce important technical improvements. Although in the AGS framework employed by us the Coulomb force can be included via the screening and renormalization method [23, 24], the present numerical results are restricted to the Coulomb-free n-^{3}H case.

We treat the nucleons as identical particles in the isospin formalism and therefore use the AGS equations for the symmetrized four-particle transition operators $\mathcal{U}_{\beta\alpha}$ as derived in Ref. [9], i.e.,

$$\begin{aligned}\mathcal{U}_{11} = {} & -(G_0\, t\, G_0)^{-1} P_{34} - P_{34} U_1 G_0\, t\, G_0\, \mathcal{U}_{11} \\ & + U_2 G_0\, t\, G_0\, \mathcal{U}_{21},\end{aligned} \tag{1a}$$

$$\mathcal{U}_{21} = (G_0\, t\, G_0)^{-1}(1 - P_{34}) + (1 - P_{34}) U_1 G_0\, t\, G_0\, \mathcal{U}_{11}, \tag{1b}$$

$$\mathcal{U}_{12} = (G_0\, t\, G_0)^{-1} - P_{34} U_1 G_0\, t\, G_0\, \mathcal{U}_{12} + U_2 G_0\, t\, G_0\, \mathcal{U}_{22}, \tag{1c}$$

$$\mathcal{U}_{22} = (1 - P_{34}) U_1 G_0\, t\, G_0\, \mathcal{U}_{12}. \tag{1d}$$

Here, $\alpha = 1$ corresponds to the $3+1$ partition (12,3)4 whereas $\alpha = 2$ corresponds to the $2+2$ partition (12)(34); there are no other distinct two-cluster partitions in the system of four identical particles.

$$G_0 = (Z - H_0)^{-1} \tag{2}$$

is the free resolvent with the complex energy parameter $Z = E + i\varepsilon$ and the free Hamiltonian H_0,

$$t = v + v G_0 t \tag{3}$$

is the pair (12) transition matrix derived from the potential v, and

$$U_\alpha = P_\alpha G_0^{-1} + P_\alpha t\, G_0\, U_\alpha, \tag{4}$$

are the symmetrized 3+1 or 2+2 subsystem transition operators. The basis states are antisymmetric under exchange of two particles in the subsystem (12) for the $3+1$ partition and in (12) and (34) for the $2+2$ partition. The full antisymmetry of the four-nucleon system is ensured by the permutation operators P_{ab} of particles a and b with $P_1 = P_{12}\, P_{23} + P_{13}\, P_{23}$ and $P_2 = P_{13}\, P_{24}$.

The scattering amplitudes for two-cluster reactions at available energy $E = \epsilon_\alpha + p_\alpha^2/2\mu_\alpha = \epsilon_\beta + p_\beta^2/2\mu_\beta$ are obtained as the on-shell matrix elements $\langle \mathbf{p}_\beta | T_{\beta\alpha} | \mathbf{p}_\alpha \rangle = S_{\beta\alpha} \langle \phi_\beta | \mathcal{U}_{\beta\alpha} | \phi_\alpha \rangle$ in the limit $\varepsilon \to +0$. Here $|\phi_\alpha\rangle$ is the Faddeev component of the asymptotic two-cluster state in the channel α, characterized by the bound state energy

$\epsilon_\alpha < 0$, the relative momentum $\mathbf{p}_\alpha$, and the reduced mass μ_α. Thus, depending on the isospin, ϵ_1 is the ground state energy of ^{3}He or ^{3}H, and ϵ_2 is twice the deuteron energy ϵ_d. $S_{\beta\alpha}$ are the symmetrization factors [9], e.g., $S_{11} = 3$. The amplitudes for breakup reactions are given by the integrals involving $\mathcal{U}_{\beta\alpha}|\phi_\alpha\rangle$ [25].

We solve the AGS equations (1) in the momentum-space partial-wave framework. The states of the total angular momentum $\mathcal{J}$ with the projection $\mathcal{M}$ are defined as $|k_x\, k_y\, k_z[l_z(\{l_y[(l_xS_x)j_x\, s_y]S_y\}J_y s_z)S_z]\,\mathcal{J}\mathcal{M}\rangle$ for the $3+1$ configuration and $|k_x\, k_y\, k_z(l_z\{(l_xS_x)j_x\, [l_y(s_ys_z)S_y]j_y\}S_z)\mathcal{J}\mathcal{M}\rangle$ for the $2+2$. Here k_x, k_y and k_z are the four-particle Jacobi momenta in the convention of Ref. [25], l_x, l_y, and l_z are the associated orbital angular momenta, j_x and j_y are the total angular momenta of pairs (12) and (34), J_y is the total angular momentum of the (123) subsystem, s_y and s_z are the spins of nucleons 3 and 4, and S_x, S_y, and S_z are channel spins of two-, three-, and four-particle system. A similar coupling scheme is used for the isospin. In the following we abbreviate all discrete quantum numbers by ν. The reduced masses associated with Jacobi momenta k_x and k_y in the partition α will be denoted by $\mu_{\alpha x}$ and $\mu_{\alpha y}$, respectively.

An explicit form of integral equations is obtained by inserting the respective completeness relations

$$1 = \sum_\nu \int_0^\infty |k_xk_yk_z\nu\rangle_\alpha k_x^2dk_x\; k_y^2dk_y\; k_z^2dk_z\; {}_\alpha\langle k_xk_yk_z\nu| \tag{5}$$

between all operators in Eqs. (1). The integrals are discretized using Gaussian quadrature rules [26] turning Eqs. (1) into a system of linear equations as described in Ref. [9]. However, in the limit $\varepsilon \to +0$ needed for the calculation of the observables the kernel of the AGS equations contains integrable singularities. At $E + i\varepsilon - \epsilon_\alpha - k_z^2/2\mu_\alpha \to 0$ the subsystem transition operator in the bound state channel has the pole

$$G_0U_\alpha G_0 \to \frac{P_\alpha|\phi_\alpha\rangle S_{\alpha\alpha}\langle\phi_\alpha|P_\alpha}{E + i\varepsilon - \epsilon_\alpha - k_z^2/2\mu_\alpha}. \tag{6}$$

Furthermore, at $E + i\varepsilon - \epsilon_d - k_y^2/2\mu_{\alpha y} - k_z^2/2\mu_\alpha \to 0$ the two-nucleon transition matrix in the channel with the deuteron quantum numbers for the pair (12) has the pole

$$t \to \frac{v|\phi_d\rangle\langle\phi_d|v}{E + i\varepsilon - \epsilon_d - k_y^2/2\mu_{\alpha y} - k_z^2/2\mu_\alpha}, \tag{7}$$

with $|\phi_d\rangle$ being the pair (12) deuteron wave function. Finally, the free resolvent (2) obviously becomes singular at $E + i\varepsilon - k_x^2/2\mu_{\alpha x} - k_y^2/2\mu_{\alpha y} - k_z^2/2\mu_\alpha \to 0$.

At energies below the three-cluster threshold only (6) singularities are present that in our previous calculations [9] were treated reliably by the subtraction technique. However, above the four-body breakup threshold all three kinds of singularities are present. Their interplay with permutation operators and basis transformations leads to a very complicated singularity structure of the AGS equations. As proposed in Ref. [17], this difficulty can be avoided by performing calculations for a set of finite $\varepsilon > 0$ values where the kernel contains no singularities and then extrapolating the results to the $\varepsilon \to +0$ limit. However, this extrapolation is only precise with not too large ε values. On the other hand, for small ε the kernel of the AGS equations, although formally being nonsingular, may exhibit a quasi-singular behavior thereby requiring dense grids for the numerical integration. This is no problem in simple model calculations with rank-one separable potential and very few channels [19] where one can use a large number of grid points. However, in practical calculations with realistic potentials and large number of partial waves necessary for the convergence one has to keep the number of integration grid points possibly small and therefore a more sophisticated integration method is needed.

We take over from Refs. [17, 19] the idea of the complex energy method and the $\varepsilon \to +0$ extrapolation procedure (analytic continuation via continued fraction) but we introduce an important technical improvement when calculating $\mathcal{U}_{\beta\alpha}$ at finite ε. We use the method of special weights for numerical integrations involving any of the above-mentioned quasi-singularities, i.e.,

$$\int_a^b \frac{f(x)}{x_0^n + iy_0 - x^n}dx \approx \sum_{j=1}^{N} f(x_j)w_j(n, x_0, y_0, a, b). \tag{8}$$

The quasi-singular factor $(x_0^n + iy_0 - x^n)^{-1}$ is separated and absorbed into the special integration weights $w_j(n, x_0, y_0, a, b)$. The set of N grid points $\{x_j\}$ where the remaining smooth function $f(x)$ has to be evaluated is chosen the same as for the standard Gaussian quadrature. However, while the standard weights are real [26], the special ones $w_j(n, x_0, y_0, a, b)$ are complex. They are chosen such that for a set of N test functions $f_j(x)$ the result (8) is exact. A convenient and reliable choice of $\{f_j(x)\}$ are the N spline functions $\{S_j(x)\}$ referring to the grid $\{x_j\}$; their construction and properties are described in Refs. [26–28]. The corresponding special weights are

$$w_j(n, x_0, y_0, a, b) = \int_a^b \frac{S_j(x)}{x_0^n + iy_0 - x^n}dx, \tag{9}$$

where the integration can be performed either analytically or numerically using sufficiently dense grid. This choice of special weights guarantees accurate results for quasi-singular integrals (8) with any $f(x)$ that can be accurately approximated by the spline functions $\{S_j(x)\}$.

In the integrals over the momentum variables one has $n = 2$, $a = 0$, and $b \to \infty$. For example, when solving the Lippmann-Schwinger equation (3) the integration variable in Eq. (8) is the momentum k_x with $x_0^2 = 2\mu_{\alpha x}(E - k_y^2/2\mu_{\alpha y} - k_z^2/2\mu_\alpha)$ and $y_0 = 2\mu_{\alpha x}\varepsilon$. Alternatively, the quasi-singularity can be isolated in a narrower interval $0 < a < b < \infty$ and treated by special weights only there.

$[\varepsilon_{\min},\varepsilon_{\max}]$	$\delta(^1S_0)$	$\eta(^1S_0)$	$\delta(^3P_0)$	$\eta(^3P_0)$	$\delta(^3P_2)$	$\eta(^3P_2)$
[1.0, 2.0]	62.63	0.990	43.03	0.959	65.27	0.950
[1.2, 2.0]	62.60	0.991	43.04	0.959	65.29	0.951
[1.4, 2.0]	62.67	0.991	43.03	0.958	65.27	0.950
[1.2, 1.8]	62.65	0.992	43.03	0.959	65.28	0.950
1.4	73.37	0.916	44.77	0.840	67.38	0.933

TABLE I. Elastic phase shifts (in degrees) and inelasticities in selected partial waves for n-^{3}H scattering at 22.1 MeV neutron energy. Results for INOY04 potential obtained using different sets of ε values ranging from $\varepsilon_{\min}$ to $\varepsilon_{\max}$ (in MeV) are compared. In the last line the predictions with $\varepsilon = 1.4$ MeV without extrapolation are given.

Other numerical techniques for solving the four-nucleon AGS equations are taken over from Ref. [9]. They include Padé summation [29] of Neumann series for the transition operators U_α and $\mathcal{U}_{\beta\alpha}$ using the algorithm of Ref. [30] and the treatment of permutation operators (basis transformations) using the spline interpolation. The specific form of the permutation operators [9] leads to a second kind of quasi-singular integrals (8) with $n = 1$, $a = -1$, $b = 1$, and the integration variable $x = \hat{\mathbf{k}}'_y \cdot \hat{\mathbf{k}}_y$ or $\hat{\mathbf{k}}'_z \cdot \hat{\mathbf{k}}_z$ being the cosine of the angle between the respective initial and final momenta.

We note that the above integration method is not sufficient in the vanishing ε limit since for $n = 1$ and $y_0 = 0$ the result of the integral (8) contains the contribution $f(x_0)\ln[(x_0+1)/(x_0-1)]$ with logarithmic singularities at $x_0 = \pm 1$. At finite small ε the result of (8) may exhibit a quasi-singular behavior. However, since the logarithmic quasi-singularity is considerably weaker than the pole quasi-singularity, at not too small ε it is sufficient to use the standard integration.

We start by applying the complex energy method with special integration weights to the n-^{3}H scattering below the three-cluster threshold where our previous results [9] obtained at real energies using subtraction technique are available for comparison. In the test calculations at 3.5 and 6.0 MeV neutron energy we find a very good agreement between the two methods, better than 0.05% for all relevant phase shifts and observables. The considered ε values range between 0.2 and 2.0 MeV, and the number of grid points is not increased as compared to the real-energy calculations [9].

Next we test the numerical reliability of our technique above the four-nucleon breakup threshold. We use a realistic dynamics, namely, the high-precision inside-nonlocal outside-Yukawa (INOY04) two-nucleon potential by Doleschall [5, 31] that reproduces experimental binding energies of ^{3}H (8.48 MeV) and ^{3}He (7.72 MeV) without an irreducible three-nucleon force. We consider a large number of four-nucleon partial waves sufficient for the convergence, i.e., $l_x, l_y, l_z, j_x, j_y, J_y \leq 4$ and $\mathcal{J} \leq 5$. Including more partial waves yields only entirely insignificant changes. There are too many numerical parameters (numbers of points for various integration grids) to demonstrate the stability of our calculations with respect to each of them separately. We found that 10 grid points are sufficient for all angular integrations but 30 to 40 grid points are needed for the discretization of Jacobi momenta. The $\varepsilon \to +0$ extrapolation yields stable results only if sufficiently small ε are considered and at each of them the respective calculations are numerically well converged. We therefore study in Fig. 1 the stability of the $\varepsilon \to +0$ results obtained via extrapolation using different ε sets ranging from $\varepsilon_{\min}$ to $\varepsilon_{\max}$ with the step of 0.2 MeV. We show the differential cross section $d\sigma/d\Omega$ and neutron analyzing power A_y for elastic n-^{3}H scattering at $E_n = 22.1$ MeV neutron energy. We find a very good agreement between the results obtained with $[\varepsilon_{\min}, \varepsilon_{\max}]$ = [1.0,2.0], [1.2,2.0], [1.4,2.0], and [1.2,1.8] MeV, confirming the reliability of our calculations. In addition, we show in Fig. 1 the predictions referring to $\varepsilon = 1.4$ MeV without extrapolation that don't have physical meaning. The difference between $\varepsilon \to +0$ and $\varepsilon = 1.4$ MeV results demonstrates the importance of the extrapolation. Furthermore, in Table I we collect the corresponding values for selected phase shifts δ and inelasticities η, i.e., we parametrize the elastic S-matrix as $s = \eta e^{2i\delta}$. As already can be expected from Fig. 1, the stability of

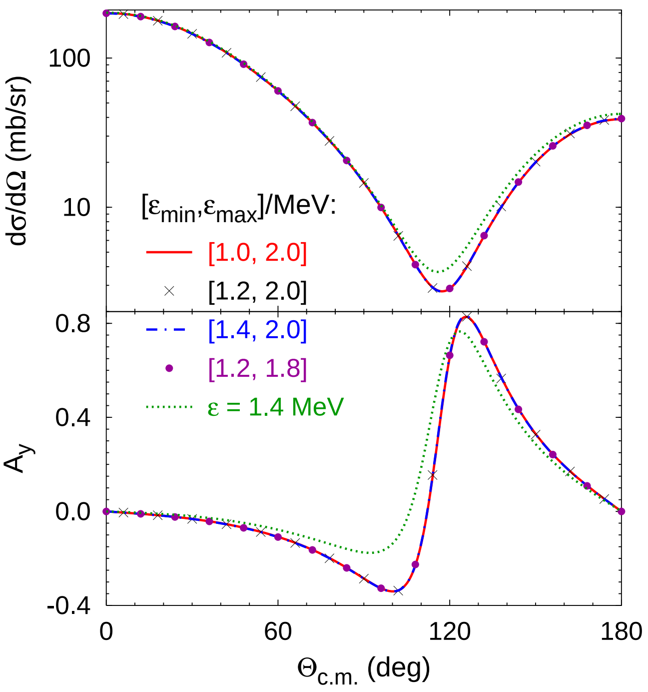

FIG. 1. (Color online) Differential cross section and neutron analyzing power for elastic n-^{3}H scattering at 22.1 MeV neutron energy as functions of c.m. scattering angle. Results obtained using different sets of ε values ranging from $\varepsilon_{\min}$ to $\varepsilon_{\max}$ with the step of 0.2 MeV are compared; they are indistinguishable. The dotted curves refer to the $\varepsilon = 1.4$ MeV calculations without extrapolation that have no physical meaning but show the importance of the extrapolation.

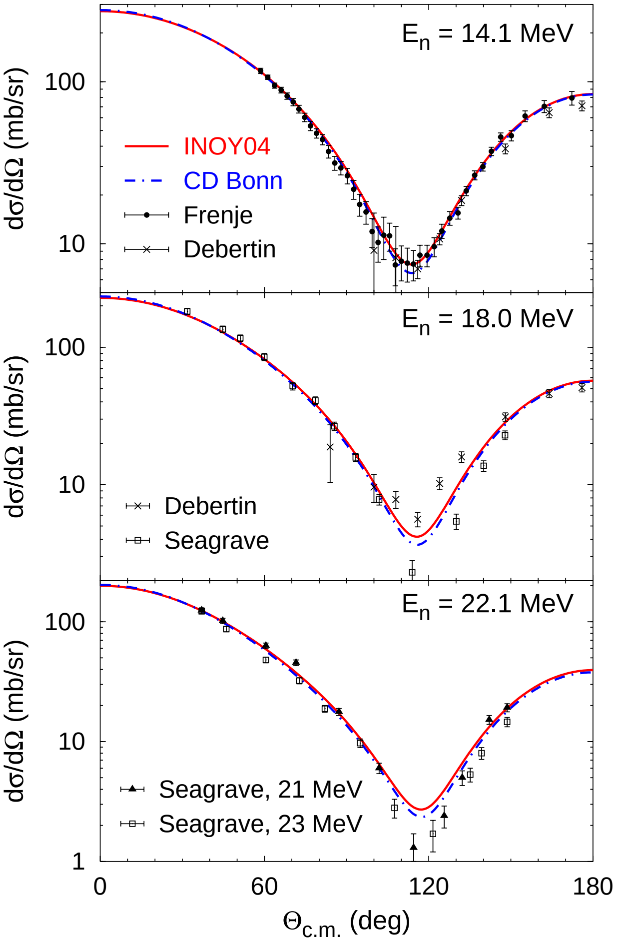

FIG. 2. (Color online) Differential cross section for elastic n-^{3}H scattering at 14.1, 18.0, and 22.1 MeV neutron energy. Results obtained with INOY04 (solid curves) and CD Bonn (dashed-dotted curves) potentials are compared with the experimental data from Refs. [22, 32, 33].

the results with respect to changes in $[\varepsilon_{\rm min}, \varepsilon_{\rm max}]$ is very good. The variations are slightly larger in the $^1S_0$ state where also the difference between the finite ε and $\varepsilon \to +0$ results is most sizable. Nevertheless, from Fig. 1 and Table I one can conclude that with a proper ε choice as few as four different ε values are sufficient to obtain the physical $\varepsilon \to +0$ results with good accuracy.

For curiosity, in $\mathcal{J} = 0$ states we performed the calculations keeping the same grids but with standard integration weights. We found that they fail completely at ε values from Table I, with the errors of the $\varepsilon \to +0$ extrapolation being up to 10 % for phase shifts and up to 25 % for inelasticity parameters. On the other hand, at large $\varepsilon > 4$ MeV the two integration methods agree well but the $\varepsilon \to +0$ extrapolation has at least one order of magnitude larger inaccuracies than those in Table I.

After establishing the reliability of our calculations we proceed to the comparison with the experimental data. In addition to the INOY04 potential we present results derived from the CD Bonn potential [34] that underbinds the ^{3}H nucleus by 0.48 MeV. In Fig. 2 we show the differential cross section for elastic neutron-^{3}H scattering at 14.1, 18.0, and 22.1 MeV neutron energy. Except for the minimum around 115 degrees, the predictions are insensitive to the choice of the potential. At $E_n = 14.1$ MeV the new data set by Frenje *et al.* [22] is described very well. Other existing data at this energy are consistent with Ref. [22] but have larger error bars; we only show the data by Debertin *et al.* [32]. At 18.0 MeV the data sets by Debertin *et al.* [32] and Seagrave *et al.* [33] are inconsistent with each other around the minimum while the theoretical predictions lie in the middle. The results at $E_n = 22.1$ MeV are compared with the data taken at 21 and 23 MeV by Seagrave *et al.* [33]. The predictions lie between the two data sets except for the minimum region. However, given the agreement between the [22] and [32] data and disagreement between the [33] and [32] data, one may question the reliability of the data by Seagrave *et al.* in the minimum region. Thus, new measurements are needed to resolve this discrepancy.

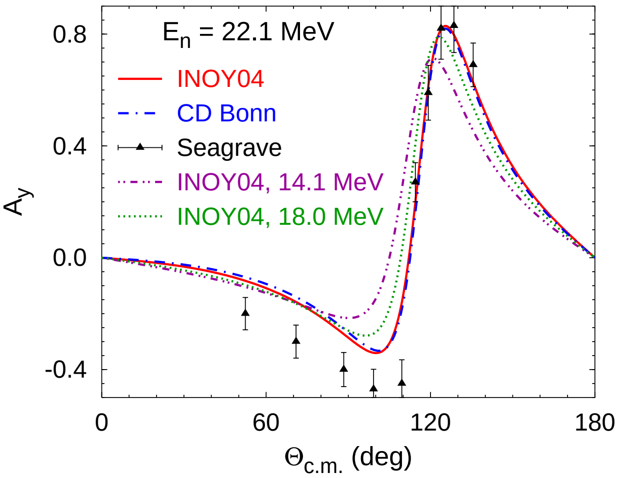

FIG. 3. (Color online) Neutron analyzing power for elastic n-^{3}H scattering. INOY04 and CD Bonn predictions at $E_n = 22.1$ MeV are compared with the data from Ref. [33]. INOY04 results at 14.1 MeV and 18.0 MeV are also shown.

In Fig. 3 we present the neutron analyzing power for elastic n-^{3}H scattering at $E_n = 22.1$ MeV. To study the energy dependence we also show INOY04 predictions at $E_n = 14.1$ and 18.0 MeV. We observe that the sensitivity to the nuclear force model and energy is considerably weaker as compared to the regime below three-cluster threshold [9, 10]. Most remarkably, in contrast to low energies where the famous p-^{3}He A_y-puzzle exists [1, 10, 35], the peak of A_y around 120 degrees is described very well but there is a discrepancy in the minimum region. This is somehow similar to the three-nucleon system where the nucleon-deuteron A_y-puzzle existing at low energies disappears as the energy increases [36].

In this work we do not calculate explicitly the breakup

	INOY04			CD Bonn			Experiment	
E_n	σ_e	σ_b	σ_t	σ_e	σ_b	σ_t	σ_t	Ref.
14.1	928	19	947	913	28	941	978 ± 70	[37]
18.0	697	41	738	689	48	737	750 ± 40	[37]
22.1	536	61	597	524	70	594	620 ± 24	[38]

TABLE II. n-^{3}H elastic σ_e, breakup σ_b, and total σ_t cross sections (in mb) at selected neutron energies (in MeV).

reactions. However, the total n-^{3}H cross section $\sigma_t = \sigma_e + \sigma_b$ with the elastic σ_e and three- and four-cluster breakup σ_b contributions is calculated using the optical theorem. The results at three considered energies are collected in Table II. The σ_t predictions are slightly lower than the experimental data from Refs. [37, 38] but in most cases they agree within error bars. The breakup cross section σ_b is most sensitive to the potential model, probably due to differences in ^{3}H binding energy and breakup threshold positions.

In summary, we performed fully converged neutron-^{3}H scattering calculations with realistic potentials above the four-nucleon breakup threshold. The symmetrized Alt, Grassberger, and Sandhas four-particle equations were solved in the momentum-space framework. We greatly improved the accuracy and the efficiency of the complex energy method by using numerical integration technique with special weights for all quasi-singularities of the pole type. The calculated elastic scattering observables show little sensitivity to the interaction model. The overall agreement with the experimental data for the elastic differential cross section and neutron analyzing power as well as for the total cross section is quite good, considerably better than in the low-energy n-^{3}H and p-^{3}He scattering. Extension of the method to other reactions in the four-nucleon system is in progress.

The author thanks R. Lazauskas and A. C. Fonseca for valuable discussions and J. A. Frenje for providing the data.

[1] M. Viviani, A. Kievsky, S. Rosati, E. A. George, and L. D. Knutson, Phys. Rev. Lett. **86**, 3739 (2001).

[2] A. Kievsky, S. Rosati, M. Viviani, L. E. Marcucci, and L. Girlanda, J. Phys. G **35**, 063101 (2008).

[3] M. Viviani, L. Girlanda, A. Kievsky, L. E. Marcucci, and S. Rosati, EPJ Web of Conferences **3**, 05011 (2010).

[4] O. A. Yakubovsky, Yad. Fiz. **5**, 1312 (1967) [Sov. J. Nucl. Phys. **5**, 937 (1967)].

[5] R. Lazauskas and J. Carbonell, Phys. Rev. C **70**, 044002 (2004).

[6] R. Lazauskas, Phys. Rev. C **79**, 054007 (2009).

[7] P. Grassberger and W. Sandhas, Nucl. Phys. **B2**, 181 (1967); E. O. Alt, P. Grassberger, and W. Sandhas, JINR report No. E4-6688 (1972).

[8] A. C. Fonseca, Lecture Notes in Physics 273 (Springer, Heidelberg, 1987), p. 161.

[9] A. Deltuva and A. C. Fonseca, Phys. Rev. C **75**, 014005 (2007).

[10] A. Deltuva and A. C. Fonseca, Phys. Rev. Lett. **98**, 162502 (2007).

[11] A. Deltuva, A. C. Fonseca, and P. U. Sauer, Phys. Lett. B **660**, 471 (2008).

[12] M. Viviani, A. Deltuva, R. Lazauskas, J. Carbonell, A. C. Fonseca, A. Kievsky, L. Marcucci, and S. Rosati, Phys. Rev. C **84**, 054010 (2011).

[13] H. M. Hofmann and G. M. Hale, Phys. Rev. C **77**, 044002 (2008).

[14] A. Deltuva and A. C. Fonseca, Phys. Rev. C **76**, 021001(R) (2007).

[15] A. Deltuva and A. C. Fonseca, Phys. Rev. C **81**, 054002 (2010).

[16] R. Lazauskas and J. Carbonell, Phys. Rev. C **84**, 034002 (2011).

[17] H. Kamada, Y. Koike, and W. Glöckle, Prog. Theor. Phys. **109**, 869L (2003).

[18] V. D. Efros, W. Leidemann, and G. Orlandini, Phys. Lett. B **338**, 130 (1994).

[19] E. Uzu, H. Kamada, and Y. Koike, Phys. Rev. C **68**, 061001(R) (2003).

[20] R. Lazauskas, private communication (2012).

[21] S. Quaglioni and P. Navratil, Phys. Rev. Lett. **101**, 092501 (2008).

[22] J. A. Frenje *et al.*, Phys. Rev. Lett. **107**, 122502 (2011).

[23] E. O. Alt and W. Sandhas, Phys. Rev. C **21**, 1733 (1980).

[24] A. Deltuva, A. C. Fonseca, and P. U. Sauer, Phys. Rev. C **71**, 054005 (2005).

[25] A. Deltuva, Phys. Rev. A **85**, 012708 (2012).

[26] W. H. Press, B. P. Flannery, S. A. Teukolsky, and W. T. Vetterling, *Numerical Recipes* (Cambridge University Press, Cambridge, 1989).

[27] C. de Boor, *A Practical Guide to Splines* (Springer Verlag, New York, 1978).

[28] W. Glöckle, G. Hasberg, and A. R. Neghabian, Z. Phys. **A305**, 217 (1982).

[29] G. A. Baker, *Essentials of Padé Approximants* (Academic Press, New York, 1975).

[30] K. Chmielewski, A. Deltuva, A. C. Fonseca, S. Nemoto, and P. U. Sauer, Phys. Rev. C **67**, 014002 (2003).

[31] P. Doleschall, Phys. Rev. C **69**, 054001 (2004).

[32] K. Debertin, E. Roessle, and J. Schott, in EXFOR database (NNDC, Brookhaven, 1967).

[33] J. Seagrave, J. Hopkins, D. Dixon, P. K. Jr., E. Kerr, A. Niiler, R. Sherman, and R. Walter, Annals of Physics **74**, 250 (1972).

[34] R. Machleidt, Phys. Rev. C **63**, 024001 (2001).

[35] B. M. Fisher, C. R. Brune, H. J. Karwowski, D. S. Leonard, E. J. Ludwig, T. C. Black, M. Viviani, A. Kievsky, and S. Rosati, Phys. Rev. C **74**, 034001 (2006).

[36] W. Glöckle, H. Witała, D. Hüber, H. Kamada, and J. Golak, Phys. Rep. **274**, 107 (1996).

[37] M. E. Battat *et al.*, Nucl. Phys. **12**, 291 (1959).

[38] T. W. Phillips, B. L. Berman, and J. D. Seagrave, Phys. Rev. C **22**, 384 (1980).